WORLD CONFERENCE ON TIMBER ENGINEERING 2025
BRISBANE, AUSTRALIA

Advancing Timber for the Future Built Environment

COMPARISON OF CRACKING PROCESS IN TROPICAL WOOD FOR MOBILITY

Riccardo Houngbegnon[1], Thomas Jailin[2], Valery Doko[3], Benoît Blaysat[4], Nicolas Sauvat[5], Joseph Gril[6], Naman Recho[7], José Xavier[8], Rostand Moutou Pitti[9]

ABSTRACT: This work addresses wood cracking for mobility. Japanese Magnolia, the wood species used for the *Lignosat* microsatellite, is compared in opening mode and mixed mode to Khaya Ivorensis, a tropical species from Benin. The study is performed with MMCG (Mixed Mode Crack Growth) specimens mounted in an Arcan system and placed in an electromechanical testing machine. Cracking parameters are studied using the LSA, a new method that accurately measures strain and displacement fields near the crack through image analysis. The energy release rate is evaluated and compared using the compliance method with imposed displacement in crack opening.

KEYWORDS: *Magnolia Obovata*, *Khaya Ivorensis*, LSA, Fracture, Tropical species

[1] Riccardo Houngbegnon, Université Clermont Auvergne, CNRS, Clermont Auvergne INP, Institut Pascal, 63000 Clermont-Ferrand, France, Université d'Abomey-Calavi, Calavi, Benin, mahugnon_riccardo.houngbegnon@etu.uca.fr

[2] Thomas Jailin, Université Clermont Auvergne, CNRS, Clermont Auvergne INP, Institut Pascal, 63000 Clermont-Ferrand, France, thomas.jailin@uca.fr

[3] Valery Doko, Université d'Abomey-Calavi, Ecole Polytechnique d'Abomey-Calavi, Calavi, Benin, dokovalery@yahoo.fr

[4] Benoît Blaysat, Université Clermont Auvergne, CNRS, Clermont Auvergne INP, Institut Pascal, 63000 Clermont-Ferrand, France, benoit.blaysat@uca.fr

[5] Nicolas Sauvat, Université Clermont Auvergne, CNRS, Clermont Auvergne INP, Institut Pascal, 63000 Clermont-Ferrand, France, nicolas.sauvat@uca.fr

[6] Joseph Gril, Université Clermont Auvergne, CNRS, Clermont Auvergne INP, Institut Pascal, 63000 Clermont-Ferrand, France, joseph.gril@uca.fr

[7] Naman Recho, Université Clermont Auvergne, CNRS, Clermont Auvergne INP, Institut Pascal, 63000 Clermont-Ferrand, France, naman.recho@uca.fr

[8] José Xavier, UNIDEMI, Department of Mechanical and Industrial Engineering, NOVA School of Science and Technology, Universidade NOVA de Lisboa, Caparica, 2829-516, Portugal, jmc.xavier@fct.unl.pt

[9] Rostand Moutou Pitti, Université Clermont Auvergne, CNRS, Clermont Auvergne INP, Institut Pascal, 63000 Clermont-Ferrand, France, CENAREST, IRT, BP 14070, Libreville, Gabon, rostand.moutou_pitti@uca.fr

https://doi.org/10.52202/080513-0200

1 – INTRODUCTION

Faced with today's environmental challenges, the use of bio-sourced materials such as wood is emerging as a sustainable solution for reducing the carbon footprint of the mobility sector [1]. As well as being renewable, this material stores carbon throughout its life cycle, thus helping to mitigate climate change. However, a better understanding of its mechanical properties is essential to optimize its use and guarantee structures that are both high-performance and durable. In recent decades, significant progress has been made in nanotechnology. With this technology, it is now possible to design and build increasingly smaller devices. Among recent innovative developments in the use of wood, *Magnolia obovata*, a Japanese species, attracted particular interest when it was used by the Japanese Space Agency (JAXA) to design the first wooden satellite called Lignosat [2], launched in October 2024, in a project aimed at reducing the amount of space debris orbiting the earth. The aim of this work is to explore new species that could replace *M. obovata* in a mobile context. *Khaya ivorensis*, a tropical African species, was chosen and compared to *M. obovata* in terms of resistance to cracking, a key criterion in the durability of mobility infrastructures.

2 – MATERIALS AND METHODS

2.1 MMCG SPECIMEN

The MMCG specimen was developed by Moutou Pitti [3], [4], making a harmonious compromise between DCB (Double Cantilever Beam) specimens with variable inertia and CTS (Compact Tension Shear) specimens. The advantage of the MMCG specimen is that the crack propagates steadily after its appearance, unlike the CTS specimen. After acquiring the *Khaya ivorensis* and *Magnolia obovata* planks, we first sawed them into thin planks. These were then laser-cut (see Fig. 1) to match the shape and dimensions of the specimens as closely as possible. We used specimens with a thickness of 12 mm and a moisture content of 12%. Fig. 2 shows the dimensions of the MMCG specimen, as well as those of the K. ivorensis and M. obovata specimens.

Figure 1: (a) Laser cutter; (b) Cutting a plank of Khaya ivorensis

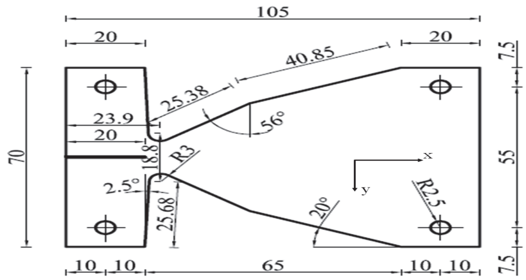

Figure 2: (a) Modified MMCG specimen; (b) Khaya ivorensis specimen; (c) Magnolia obovata specimen

The density of the *Magnolia obovata* used in our tests is 464 kg/m^3 and that of *Khaya ivorensis* is 777 kg/m^3.

2.2 LSA METHOD

Localized Spectral Analysis (LSA) is a technique used to extract displacement and deformation fields from images, based on a spectral analysis. LSA consists first in calculating the windowed Fourier transform (WFT) of the image of the periodic pattern for a given frequency, which is the nominal frequency of the periodic pattern [5]. This frequency is denoted by:

$$f = \frac{1}{p} \qquad (1),$$

where p is the pitch of the pattern. The Gaussian window is the best compromise between the different constraints [5]. The function defining this Gaussian window is given by the following equation:

$$g(x, y) = \frac{1}{2\pi\sigma^2} e^{\left(-\frac{x^2+y^2}{2\sigma^2}\right)} \qquad (2),$$

where σ is the standard deviation of the Gaussian. Displacements along the x and y directions, designated by u_x and u_y, respectively, are proportional to the phase change between the current (or distorted) image and the reference image [6]. Thus, we have:

$$\underline{u}(\underline{x}) = -\frac{p}{2\pi}\left(\underline{\Phi}^{cur}\left(\underline{x} + \underline{u}(\underline{x})\right) - \underline{\Phi}^{ref}(\underline{x})\right) \qquad (3),$$

where u represents the displacement vector of the components u_x and u_y in the base (x, y). $\underline{\Phi}^{cur}$ and $\underline{\Phi}^{ref}$ denote the current and reference phase vectors of the components Φ_x^{ref}, Φ_y^{ref} and Φ_x^{cur}, Φ_y^{cur} in the (x, y) base, respectively. To use the LSA, a checkerboard pattern must be engraved on the surface of the test specimen. The checkerboard is engraved after two coats of white paint have been applied to the surface of the specimen. In our case, we used Spartex RAL 9010 paints (Fig. 3a) and an etching machine as shown in Fig. 4.

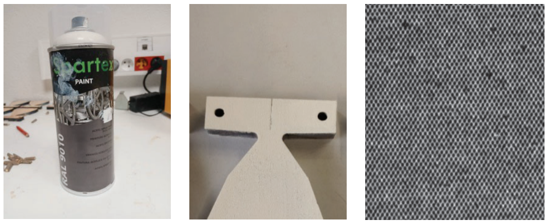

(a) (b) (c)

Figure 3: (a) Paint; (b) Specimen surface after painting; (c) Checkerboard

Figure 4: Engraving machine

Two types of checkerboard were used in our work. Each was engraved on a separate side of the test specimen, enabling us to visualize two zones. A 30 µm - square width checkerboard on the first side and a large 70 µm - square width checkerboard on the second. The 70 µm checkerboard enabled us to visualize the entire surface of the specimen. The 30 µm checkerboard enabled us to visualize the surface around the crack. The characteristics of the two checkerboards are shown in Tab. 1.

Table 1: Small and large checkerboard features

Features	Small checkerboard (cm)	Large checkerboard
Pattern size (µm)	30	70
Laser power	70	40
Sweep speed	3600	5600
Pulse frequency	60	40
Number of repetitions	20	10

2.3 CRACKING TEST

A steel Arcan system was used for the tests. The shape of the Arcan system leaves a gap in the middle, so that the checkerboard engraved on the specimens is visible; it is suitable for all stress modes, including mixed mode with its different stress angles (see Fig. 5). The device has been designed to be used for testing CTS specimens in open mode (mode 1) and MMCG specimens in mode 1 and mixed mode [7]. The Arcan system is made of high-tensile steel.

A Zwick/Roel type tension-compression machine, with a loading capacity of 200kN and mounted with a 50kN load, was used to carry out the tests. Two cameras mounted on tripods (one on each side of the test specimen) were used to photograph images of the checkerboard during the tests. Illuminated spotlights were used to enhance the illumination of the test specimen surfaces and ensure sharp images. Fig. 6 shows the complete experimental set-up. The Arcan steel device used to load the specimens is also visible. The test machine's movable jaw (upper jaw) is controlled by a 0.05mm/s imposed displacement. It is fitted with a force transducer.

Figure 5: Specimen in Arcan system

Fig. 6: Experimental set-up

https://doi.org/10.52202/080513-0200

3 – RESULTS

Following our cracking tests, we obtained force-displacement curves for all the specimens tested. Those obtained in crack-opening mode are shown in Fig.8. These curves clearly show that the maximum forces obtained at fracture for *Khaya ivorensis* specimens are superior to those obtained for *Magnolia obovata*. The force-displacement curves obtained for *Magnolia obovata* and *Khaya ivorensis* show distinct mechanical behaviors. *Magnolia obovata* shows lower displacements, with a maximum load reaching around 235 N. The curves show a gradual rise followed by fluctuations, probably due to microcracks before failure. Failure occurs relatively abruptly, suggesting a more pronounced fragility. *Khaya ivorensis*, on the other hand, shows significantly higher displacements, reaching around 5 to 6 mm, with maximum loads approaching 600 N for some samples. The curves show a more gradual and sustained rise, with more extensive post-peak behavior, indicating a better capacity to absorb energy before failure. These results suggest that *Khaya ivorensis* has greater ductility and mechanical strength than *Magnolia obovata*, which appears stiffer but more brittle.

The LSA method then gave us the displacement and deformation maps. The displacement maps enable us to determine crack opening values, while the deformation maps allow us to obtain the position of the crack tip. These two parameters are essential for determining the energy release rate using the imposed displacement compliance method, the formula for which is given by the following equation [8].

$$G_C = \frac{(F_{Ci})^2}{2b} x \left(\frac{\Delta C}{\Delta a}\right)_d \quad (4),$$

with F_{Ci} the critical forces corresponding to the peaks recorded on the force-crack opening curves, $\Delta C = U_i / F_{Ci}$ the compliance, U_i the crack opening, Δa the crack length and b the specimen thickness.

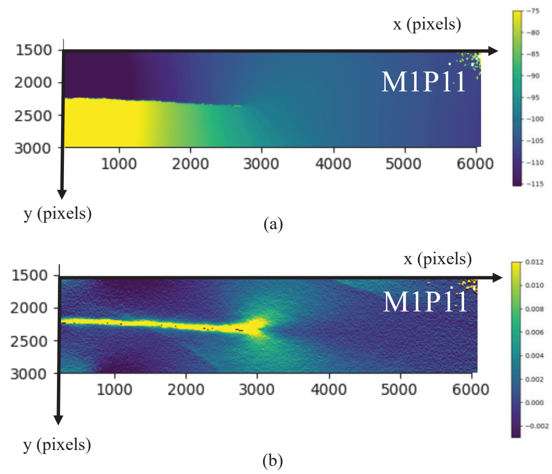

Figure 7: (a) Typical displacement curve; (b) Typical deformation curve

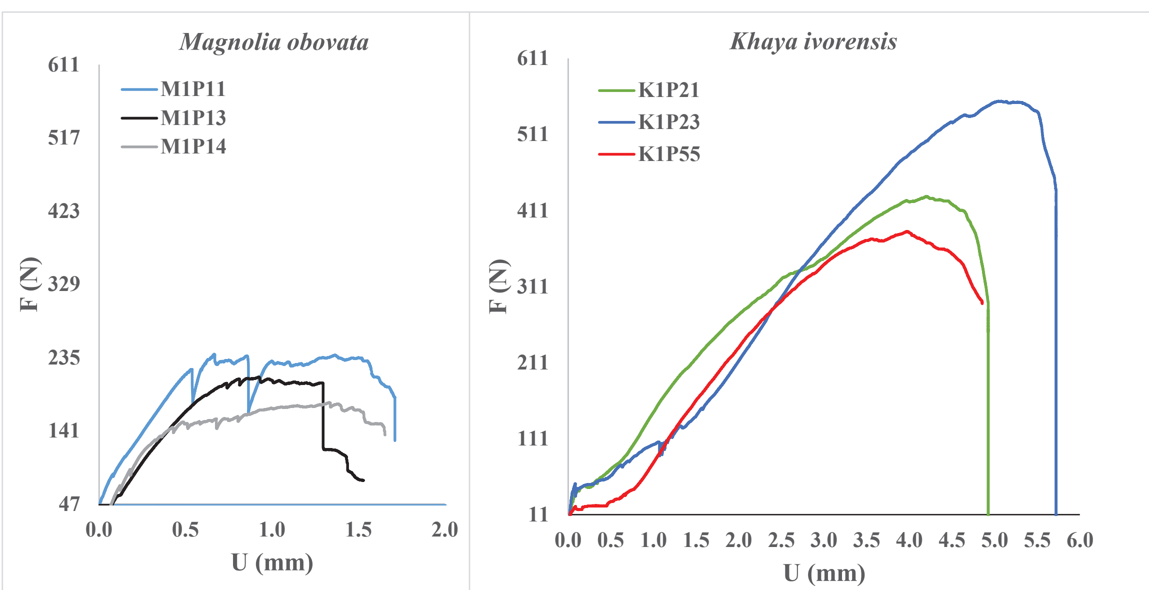

Figure 8: Force-displacement curves for Khaya ivorensis and Magnolia obovata

Tab. 2 and Tab. 3 shows respectively the minimum and maximum energy release rate values for Magnolia and Khaya specimens. According to these tables, the energy release rate values of *Khaya ivorensis* are higher than those of *Magnolia obovata*, both in terms of minimum and maximum values. In fact, the average G_{min} values for Magnolia and Khaya are 148 J/m² and 436 J/m² respectively, while the average G_{max} values are 247 J/m² and 1101 J/m² respectively. The values obtained are consistent with the density orders of the two species. Remember that the density of the *Magnolia obovata* used in our tests is 464 kg/m3 and that of *Khaya ivorensis* is 777 kg/m3. This difference could partly explain the differences in values observed between the two species, both in terms of breaking forces and energy release rates. This confirms the results obtained by [7] with three tropical tree species of different densities.

Table 2: Maximum and average energy restitution rates for Magnolia and Khaya

Species	Specimens	Max value	Average
Magnolia obovata	M1P11	286	247
	M1P12	222	
	M1P14	232	
Khaya ivorensis	K1P21	1208	1101
	K1P23	1489	
	K1P55	664	

Table 3: Maximum and average energy restitution rates for Magnolia and Khaya

Species	Specimens	Min value	Average
Magnolia obovata	M1P11	198	148
	M1P12	128	
	M1P14	118	
Khaya ivorensis	K1P21	235	436
	K1P23	740	
	K1P55	332	

4 – CONCLUSION

This paper proposes a comparative study between the cracking characteristics of *Khaya ivorensis* and *Magnolia obovata* for a potential use of *Khaya ivorensis* in mobility application. The data obtained allow us to say that the two species compared show good performance in terms of resistance to cracking, especially *K. ivorensis*. The energy release rate values obtained are consistent with the density orders of the two species. It should also be noted that the use of *K. ivorensis* as a mobility material would greatly enhance the value of this little-known species. For future research, it would be useful to calculate the cracking parameters of *Khaya ivorensis*, taking into account variations in humidity and temperature. Consideration should also be given to assessing the impact of ageing and repeated stress on the durability of *K. ivorensis*.

4 – ACKNOWLEDGMENT

The authors would like to thank the CIT ITPS Cap2025 program (UCA) and the ANR via the WoodMob, Emergence and DIAMWOOD projects for supporting this work.

7 – REFERENCES

[1] B. Castané, C. Bouvet, J. Serra, F. Eyma et A. Cantarel, «Wood, a material for sustainable mobility ?,» *CEMA,* vol. 2, pp. 1-4, 2022.

[2] K. Tsuji, Y. Sugahara et M. Nagatomo, «Développement d'un satellite artificiel en bois utilisant Magnolia obovata,» 2021.

[3] R. Moutou Pitti, «Decoupling of mixed-mode fracture in orthotropic viscoelastic materials: Modeling and experimentation,» *C.R. Mecanique,* vol. 336, pp. 744-749, 2008.

[4] F. Dubois, «Modélisation du comportement mécanique des mileiux viscoélastiques fissurés : Application au matériau bois,» Limoges, 1997.

[5] M. Grédiac, B. Blaysat et F. Sur, «Extracting Displacement and Strain Fields from Checkerboard Images with the Localized Spectrum Analysis,» *Society for Experimental Mechanics,* vol. 59, pp. 207-218, 2018.

[6] Y. Surrel, «Moire' and grid methods : a signal-processing approach,» *Interférométrie '94 : photomechanics,* vol. 2342, 1994.

[7] B. Odounga, «Study of cracking in tropical woods by field measurements,» *HAL Open Science,* pp. 100-125, 2018.

[8] A. Pirondi et C. Dalle Donne, «Characterisation of ductile mixed-mode fracture with the crack-tip displacement vector,» *Engineering Fracture Mechanics,* vol. 68, pp. 1385-1402, 2001.

https://doi.org/10.52202/080513-0200